DALTON

η^2-Sulfenamido and -selenamido complexes of titanium, zirconium, molybdenum and tungsten

Danielle M. Hankin,[a] Andreas A. Danopoulos,[a] Geoffrey Wilkinson,*[,a] Tracy K. N. Sweet[b] and Michael B. Hursthouse*[,b]

[a] *Johnson Matthey Laboratory, Chemistry Department, Imperial College, London SW7 2AY, UK*
[b] *Department of Chemistry, University of Wales Cardiff, PO Box 912, Cardiff CF1 3TB, UK*

The interaction of $TiCl_4$ with $LiN(Bu^t)SR$ (R = Ph or $C_6H_2Me_3$-2,4,6) gave the sulfenamido complexes $TiCl_2(\eta^2\text{-}Bu^tNSR)_2$. Interaction of $ZrCl_4$ with 3 equivalents of $LiN(Bu^t)SPh$ produced $ZrCl(\eta^2\text{-}Bu^tNSPh)_3$ while $ZrCl_4(tht)_2$ (tht = tetrahydrothiophene) with 5 equivalents gave the homoleptic $Zr(\eta^2\text{-}Bu^tNSPh)_4$. From $ZrCl_2(\eta^5\text{-}C_5H_5)_2$ only $ZrCl(\eta^5\text{-}C_5H_5)_2(\eta^2\text{-}Bu^tNSPh)$ **5** is obtained. Using as starting materials $MO_2Cl_2(dme)$ (dme = 1,2-dimethoxyethane, M = Mo or W), $MoCl_2(NBu^t)_2$ and $WCl_2(NBu^t)_2(py)_2$ (py = pyridine), interactions with $LiNBu^tSPh$ gave η^2-sulfenamido compounds such as $MoO_2(\eta^2\text{-}Bu^tNSPh)_2$. The selenium analogue of the tungsten compound, *i.e.* $W(NBu^t)_2(\eta^2\text{-}Bu^tNSePh)_2$ has been made by interaction of $Li_2W(NBu^t)_4$ with PhSeBr. Where study was possible, NMR spectra over a temperature range indicate that invertomers and isomers occur. Six compounds have been structurally characterised by X-ray diffraction. In all cases the sulfenamido ligands are η^2 bonded and the geometry about the N atoms is planar.

Sulfenamides of the general type RR′NSR″ have long been known[1] and found to have useful applications.[2-4] As referenced by Noble and co-workers[4] there are scattered reports of metal complexes of the neutral sulfenamides, but few with ligands of the anionic sulfenamido species of type $RR'NS^-$ such as a molybdenum complex with $\mu\text{-}SNH_2^-$ bridges described by Noble. In extending earlier studies[5] on the interaction of halides such as $AlCl_3$ or PCl_3 with $Li_2W(NBu^t)_4$, it was discovered that interaction with PhSCl gave a complex with a new type of sulfenamide ligand, $PhSNBu^{t-}$, as described in a communication.[6] Ligands of this type can be compared to hydrazide(1−) and hydroxyamide(1−) ligands, $RR'NNR''^-$ and $RNOR'^-$.[7] In such sulfenamide ligands delocalisation of charge can occur, *e.g.* $R\ddot{N}^- - \ddot{S}R \longleftrightarrow RN{=}S^-R$, and they could act by use of the appropriate lone pairs. Changing the substituents on N or S can, potentially, alter the reactivity and structure of the complexes.

This first paper expands on the communication, describing the more general synthetic reaction of MX_n and RN(Li)SR′ and its application to chloride compounds of Ti, Zr, Mo and W. Future papers will describe compounds of other transition metals such as Cr, Ru, Co and Ni where, *inter alia*, N–S cleavage reactions have been observed. Analytical and physical data for new compounds are given in Table 1.

Results and Discussion

Since the syntheses depend on the reaction of RN(H)SR′ with $LiBu^n$ to give the lithium reagent, a brief comment on the preparation of these sulfenamides is appropriate. Although $Bu^tN(H)SPh$ has been made by interaction of NH_2Bu^t with PhSOMe[8] we have prepared this by a modification of the Zincke method,[1] namely the interaction of 2 equivalents of NH_2Bu^t with PhSCl in diethyl ether.[9] The reaction probably involves nucleophilic attack of the amine on the electrophilic sulfur and the mechanism has been discussed.[9] This procedure has also been used for sulfenanilides using aniline or anilines with electron-withdrawing substituents.[10] Sometimes in reactions under N_2 red oils were formed making isolation of the anilide difficult; best yields are obtained under dry air or oxygen. Although a radical mechanism for the synthesis is not proven,[9] this cannot be dismissed.

We have been unable to obtain the more unstable selenamides such as the known $Bu^tN(H)SePh$[11] in a pure state. The interactions of NH_2Bu^t with PhSeBr, $Bu^tN(H)Li$ with PhSeBr and $Bu^tN(H)Li$ with PhSeSePh in various ratios of the reactants in Et_2O and tetrahydrofuran (thf) and at different temperatures were studied. There was always contamination by $(PhSe)_2$ (detected by ^{77}Se NMR spectroscopy and by GC–mass spectrometric analysis) which made purification of the thermally unstable selenamides impossible. However, the interaction of 2,4,6-$Me_3C_6H_2SeBr$, with an excess of NH_2Bu^t under specific conditions (see Experimental section) gives 2,4,6-$Me_3C_6H_2SeN(H)Bu^t$ contaminated with only minor quantities (< 7% according to ^{77}Se NMR spectroscopy) of $(2,4,6\text{-}Me_3C_6H_2Se)_2$. Deprotonation by $LiBu^n$ in light petroleum gives essentially pure 2,4,6-$Me_3C_6H_2SeN(Bu^t)Li$ allowing syntheses of metal complexes; these will be reported in a subsequent paper.

Deprotonation of primary sulfenamides with strong bases $LiBu^n$, LiMe, *etc.*, in light petroleum, or KH in thf, gives the lithium or potassium sulfenamido species. These are white, extremely air-sensitive, probably polymeric powders that are insoluble in hydrocarbons [slightly soluble in toluene in the case of $Bu^tN(Li)SPh$], but soluble in tetrahydrofuran to give yellow solutions.

Titanium complexes

The interaction of $TiCl_4$ with 2–4 equivalents of $LiN(Bu^t)SPh$ in toluene leads, after work-up, to isolation of $TiCl_2(\eta^2\text{-}Bu^tNSPh)_2$ **1** in moderate yields after crystallisation from light petroleum. This is extremely sensitive to moisture and decomposes above 95 °C. The following points may be noted: (*i*) no products can be obtained either when carrying out the reaction in co-ordinating solvents, *e.g.* thf or Et_2O, or when using $TiCl_4(thf)_2$ (this is probably due to the difficulty of displacing hard donors on a hard metal by a soft sulfur atom); (*ii*) no other products are isolated or detected by varying the sulfenamide to metal ratio within the range 4–1 : 1 (*cf.* zirconium compounds below).

The spectroscopic and analytical data are in agreement with the structure determined by X-ray crystallography [Fig. 1(*a*); selected bond lengths and angles in Table 2]. The geometry of

Table 1 Analytical and physical data for new compounds

Compound	Colour	M.p./°C	Analysis (%)[a] C	H	N
1 $TiCl_2(\eta^2\text{-}Bu^tNSPh)_2$	Yellow	95 (decomp.)	49.9 (50.1)	5.9 (5.9)	5.9 (5.9)
2 $TiCl_2(Bu^tNSC_6H_2Me_3\text{-}2,4,6)_2$	Orange	176–179	55.4 (55.7)	7.2 (7.1)	5.0 (4.8)
3 $ZrCl(\eta^2\text{-}Bu^tNSPh)_3$	Colourless	67 (decomp.)	53.8 (54.0)	6.6 (6.3)	5.9 (6.3)
4 $Zr(\eta^2\text{-}Bu^tNSPh)_4$[b]	Colourless	280 (decomp.)			
5 $ZrCl(\eta^5\text{-}C_5H_5)_2(\eta^2\text{-}Bu^tNSPh)$	Yellow	137–139	54.7 (55.0)	5.5 (5.5)	3.1 (3.2)
6 $MoO_2(\eta^2\text{-}Bu^tNSPh)_2$	Pale green	185–187	48.6 (49.2)	5.5 (5.8)	5.5 (5.7)
7 $WO_2(\eta^2\text{-}Bu^tNSPh)_2$	Pale yellow	198–200	41.5 (41.7)	4.9 (4.9)	4.8 (4.9)
8 $Mo(NBu^t)_2(\eta^2\text{-}Bu^tNSPh)_2$[c]	Pale yellow	187–188	55.9 (56.2)	7.6 (7.7)	9.5 (9.4)
10 $MoCl(NBu^t)_2(Bu^tNSC_6H_2Me_3\text{-}2,4,6)$	Green	170–174	52.0 (50.8)	7.7 (7.7)	8.4 (8.5)
11 $W(NBu^t)_2(\eta^2\text{-}Bu^tNSePh)_2$	Colourless	162–164	43.1 (43.1)	5.7 (5.9)	7.2 (7.2)

[a] Calculated values in parentheses. For mass spectra see Experimental section. [b] No analytical data, see text. [c] For $W(NBu^t)_2(Bu^tNSPh)_2$ **9** see ref. 6 and Experimental section.

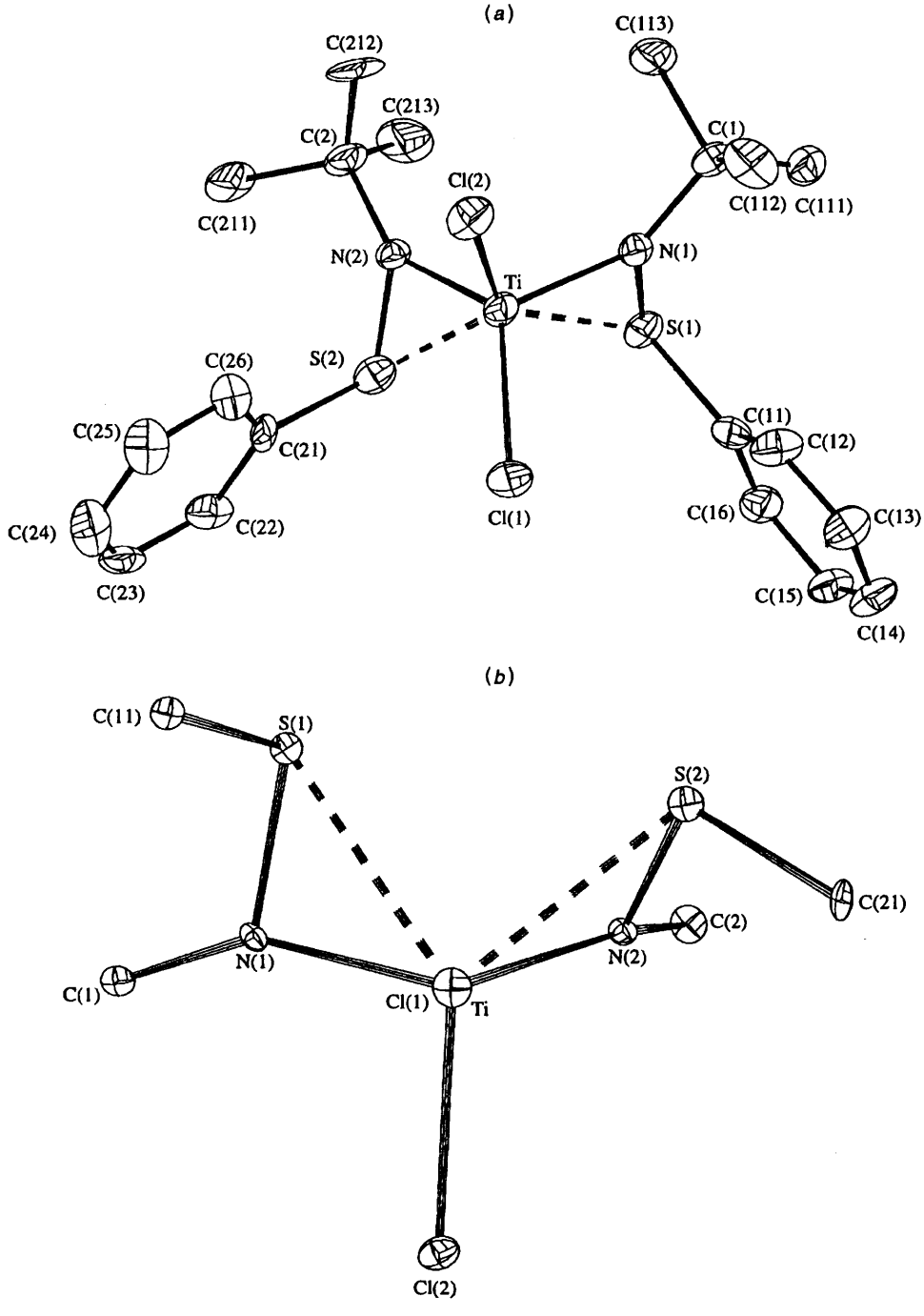

Fig. 1 Structure of $TiCl_2(\eta^2\text{-}Bu^tNSPh)_2$ **1** (*a*) and its core viewed along the Cl(1)–Ti bond (*b*)

Table 2 Selected bond lengths (Å) and angles (°) for $TiCl_2(\eta^2$-$Bu^tNSPh)_2$ **1**, with estimated standard deviations (e.s.d.s) in parentheses

Ti–N(1)	1.902(7)	S(1)–N(1)	1.692(7)
Ti–N(2)	1.900(8)	S(1)–C(11)	1.765(10)
Ti–S(1)	2.499(3)	S(2)–N(2)	1.679(7)
Ti–S(2)	2.530(3)	S(2)–C(21)	1.798(9)
Ti–Cl(1)	2.295(4)	N(1)–C(1)	1.516(11)
Ti–Cl(2)	2.270(3)	N(2)–C(2)	1.503(12)
N(1)–Ti–S(1)	42.6(2)	Cl(1)–Ti–Cl(2)	100.2(1)
N(1)–Ti–Cl(1)	112.9(3)	C(1)–N(1)–S(1)	121.6(6)
N(1)–Ti–N(2)	113.1(3)	C(1)–N(1)–Ti	148.3(5)
N(1)–Ti–S(2)	124.7(2)	S(1)–N(1)–Ti	87.9(3)
N(1)–Ti–Cl(2)	96.2(2)	C(11)–S(1)–N(1)	106.5(4)
N(2)–Ti–S(1)	99.1(2)	C(11)–S(1)–Ti	111.6(3)
N(2)–Ti–Cl(1)	126.5(2)	N(1)–S(1)–Ti	49.5(3)
N(2)–Ti–S(2)	41.6(2)	C(2)–N(2)–S(2)	119.8(6)
N(2)–Ti–Cl(2)	100.5(2)	C(2)–N(2)–Ti	147.8(6)
S(1)–Ti–Cl(1)	96.7(1)	S(2)–N(2)–Ti	89.8(4)
S(1)–Ti–S(2)	86.9(1)	C(21)–S(2)–N(2)	107.2(4)
S(1)–Ti–Cl(2)	138.8(1)	C(21)–S(2)–Ti	108.0(3)
S(2)–Ti–Cl(1)	89.2(1)	N(2)–S(2)–Ti	48.7(3)
S(2)–Ti–Cl(2)	130.4(1)		

the complex is best described in terms of a core $TiCl_2N_2$ tetrahedral geometry with two additional, weak Ti···S interactions. The Ti–N distances are equal within error and are short enough to suggest the possibility of some $N_p \rightarrow Ti_{d_\pi}$ bonding. The nitrogens are planar, as is typically found in organoamides of low d-electron-count transition metals. The Ti–Cl bonds show a small but significant difference of 0.025(5) Å, but have lengths which are typical for tetrahedral titanium(IV) chloro complexes. The Ti···S distances also differ slightly [0.031(4) Å], but this is not too surprising in view of their presumed weakness, judging by their lengths. These are *ca.* 0.2 Å longer than might be expected from the covalent radii sum. That some Ti···S interaction exists is indicated by the tilting of the co-ordinating amide part of the ligand, where the *exo* Ti–N–C angles in the two ligands are *ca.* 148°. An analogous geometry was found in the compound $W(NBu^t)_2(\eta^2$-$Bu^tNSPh)_2$ previously described.[6] Consideration of covalent radii would predict a value of *ca.* 1.74 Å for a nitrogen–sulfur single bond, so the values found, 1.68–1.69(1) Å indicate some degree of multiple-bond character and thus a contribution to the bonding from the form $RN{=}S^-R'$; this would give the sulfur enhanced donor capability. One further feature of the structure which is worthy of mention is the actual conformation of the sulfenamide ligand. Whilst the nitrogen is planar, the sulfur is pyramidal, and the torsion angles about the N–S bond involving the carbons are *ca.* 90°. This feature has implications for the directions of the sulfur donor orbitals, and the pyramidality of the sulfur gives rise to the possibility of invertomers in respect of the metal–sulfur interactions. Detailed assessment of the molecular structure reveals an intriguing situation. First, inspection of Fig. 1(*a*) shows that, in relation to the $TiCl_2$ plane as a reference element, the S–N vectors of the two sulfenamide ligands are directed in approximately the same direction, giving what might be termed a *Z* configuration. This contrasts with the structure of the tungsten complex mentioned above,[6] which, on a similar basis, but using the metal and the two imido nitrogens to define the reference plane, has the two sulfenamide N–S vectors orientated to give an *E* configuration.

For the previous tungsten compound[6] we based our description on a core $W(N_{imido})_2(N_{sulf})_2$ tetrahedron, with the weak sulfur interactions being directed to face capping positions. Analysis of the present structure shows a different situation, in addition to the *E*/*Z* configurations. Fig. 1(*b*) shows the titanium complex viewed along one of the Cl–Ti bonds and highlights a significant difference in the orientation of the two N–S bonds with respect to the Cl_2N_2 tetrahedron. The N(1)–S(1) vector is directed away from the observer parallel to the Cl(2)–Ti bond view direction and this points one of the possible lone-pair orientations (which could be either an sp^3 hybrid or a pure p orbital) towards the centre of the face Cl(1), N(1), N(2). The N(2)–S(2) vector also points downwards, but is skewed relative to the direction of view. Examination of a model shows that this orientation directs one of the sulfur lone pairs towards the N(2)–Cl(1) *edge* of the tetrahedron. It is pertinent that in the classical representation of tetrahedral, sp^3 stereochemistry, where the ligands sit at two mutually orthogonal pairs of cube corners, the $d_{x^2-y^2}$, d_{z^2} lobes are directed to the edges of the tetrahedron, and the d_{xy}, d_{yz}, d_{zx} to the faces. In the present complex, therefore, interaction of the co-ordinating sulfur lone pairs with titanium d orbitals would be possible in both cases.

The ^1H NMR spectrum of complex **1** in $[^2H_8]$toluene at 25 °C consists of two Bu^tN bands in a 1:1 ratio, plus bands due to aromatic protons. The former collapse at 110 °C to a broad singlet and this change is reversed on cooling. Assuming the solid-state structure to persist in solution, two magnetically inequivalent *tert*-butyl groups are expected (C_1). Raising the temperature could result in fast sulfur inversion[12] (*cf.* the inversion of the S and N in the μ-SNH_2 species[4]) which would render the Bu^tN groups magnetically equivalent (effective symmetry C_s) in the fast-exchange limit. There is no evidence for the presence of another isomer in solution. The reversibility of the changes with temperature observed in the NMR spectra suggests that a second dynamic process is not observed. This would have been amido rotation following the weakening of the Ti–S bond due to pyramidal inversion had the geometry at N not been planar as found in all of the complexes discussed in this paper.

The complex $TiCl_2(Bu^tNSC_6H_2Me_3$-2,4,6$)_2$ **2**, was made in a way similar to **1**. Its identity was established by ^1H NMR and analytical data. The mass spectrum [electron impact (EI) or fast atom bombardment (FAB)] did not give the molecular ion.

Zirconium complexes

The interaction of $ZrCl_4$ with $LiN(Bu^t)SPh$ produces isolable products only when aromatic solvents are used. Thus in toluene, 3 equivalents of lithium reagent give moderate yields of $ZrCl(\eta^2$-$Bu^tNSPh)_3$ **3** after crystallisation from light petroleum–toluene or light petroleum. The compound is thermally stable but extremely air-sensitive. The spectroscopic and analytical data are all in agreement with the structure as determined by X-ray diffraction which is shown in Fig. 2(*a*); selected bond lengths and angles are given in Table 3.

The co-ordination geometry can again be described in terms of a tetrahedral core co-ordination, this time comprising one chlorine and three nitrogens. Fig. 2(*b*) shows the co-ordination sphere plus first carbons, and the way in which the sulfurs are positioned relative to the tetrahedron. Examination of models and analysis of torsion angles indicates that the lone pair from S(1) is directed towards the N(1), N(2), N(3) face, from S(2) towards the N(2), N(3) edge and from S(3) towards the Cl, N(1), N(3) face. A rigid structure of this type would therefore give three chemically distinct ligands. Examination of Table 3 shows some variations in Zr–N, Zr···S and N–S distances which may be a result of the different bonding situations.

The ^1H NMR spectrum of complex **3** at *ca.* 25 °C shows four Bu^tN peaks in a 1:1:1:1 ratio (with additional aromatic peaks). Although a complete analysis of the spectrum was not attempted this suggests the presence of more than one isomer. Inversion of all three S atoms will complicate the picture even further.

Monitoring the $ZrCl_4$ reaction with $LiNBu^tSPh$ by NMR spectroscopy shows the presence of an additional compound in solution at high ligand-to-metal ratios. Although we have not

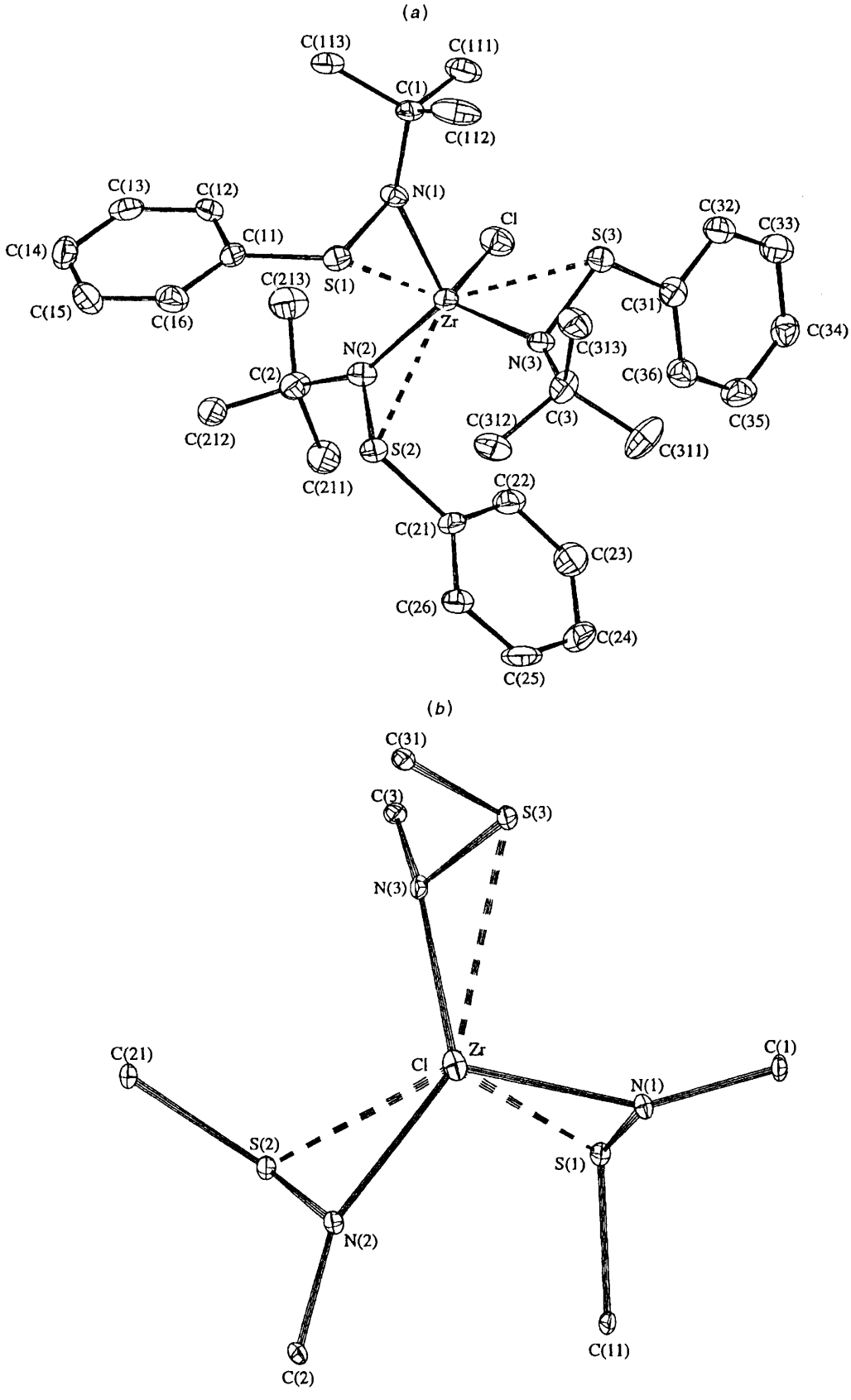

Fig. 2 Structure of $ZrCl(\eta^2\text{-Bu}^t\text{NSPh})_3$ **3** (*a*) and its core viewed along the Cl–Zr bond (*b*)

isolated this from the $ZrCl_4$ reaction, it can be obtained by interaction of the tetrahydrothiophene compound, $ZrCl_4(tht)_2$, which is much more soluble in toluene, with *ca.* 5 equivalents of the lithium reagent. Attempts to obtain meaningful analytical data were unsuccessful and mass spectra (EI, FAB) did not show the parent ion. The structure was however determined by X-ray crystallography and a diagram of $Zr(\eta^2\text{-Bu}^t\text{NSPh})_4$ **4** is shown in Fig. 3(*a*); bond lengths and angles are given in Table 4. This compound has a symmetrical structure which may be conveniently described in terms of a distorted dodecahedral geometry. The main distortions involve a twisting of the two trapezoidal planes which make up this geometry away from the ideal 90 to 64.4°, separation of the two planes resulting in loss of their mutual intersection and then twisting of the N,S chelating

Table 3 Selected bond lengths (Å) and angles (°) for $ZrCl(\eta^2\text{-}Bu^tNSPh)_3$ **3**, with e.s.d.s in parentheses

Zr–N(1)	2.092(3)	S(1)–C(11)	1.792(4)
Zr–N(2)	2.107(3)	S(2)–N(2)	1.659(3)
Zr–N(3)	2.119(3)	S(2)–C(21)	1.803(4)
Zr–S(1)	2.686(1)	S(3)–N(3)	1.701(4)
Zr–S(2)	2.649(1)	S(3)–C(31)	1.800(4)
Zr–S(3)	2.702(2)	N(1)–C(1)	1.513(5)
Zr–Cl	2.457(2)	N(2)–C(2)	1.513(5)
S(1)–N(1)	1.686(3)	N(3)–C(3)	1.497(5)
N(1)–Zr–Cl	102.6(1)	Cl–Zr–S(3)	83.7(1)
N(1)–Zr–N(2)	115.3(1)	C(1)–N(1)–S(1)	117.9(2)
N(1)–Zr–N(3)	104.9(1)	C(1)–N(1)–Zr	145.8(3)
N(1)–Zr–S(1)	38.9(1)	S(1)–N(1)–Zr	89.9(2)
N(1)–Zr–S(2)	122.1(1)	C(2)–N(2)–S(2)	118.6(3)
N(1)–Zr–S(3)	91.4(1)	C(2)–N(2)–Zr	151.9(3)
N(2)–Zr–Cl	89.2(1)	S(2)–N(2)–Zr	88.6(1)
N(2)–Zr–N(3)	126.7(1)	C(3)–N(3)–S(3)	116.7(3)
N(2)–Zr–S(1)	95.0(1)	C(3)–N(3)–Zr	148.8(3)
N(2)–Zr–S(2)	38.8(1)	S(3)–N(3)–Zr	89.3(2)
N(2)–Zr–S(3)	153.3(1)	C(11)–S(1)–N(1)	107.1(2)
N(3)–Zr–Cl	115.4(1)	N(1)–S(1)–Zr	51.2(1)
N(3)–Zr–S(1)	95.2(1)	C(11)–S(1)–Zr	111.9(1)
N(3)–Zr–S(2)	90.5(1)	C(21)–S(2)–N(2)	108.2(2)
N(3)–Zr–S(3)	39.0(1)	N(2)–S(2)–Zr	52.7(1)
S(1)–Zr–Cl	138.0(1)	C(21)–S(2)–Zr	104.7(2)
S(1)–Zr–S(2)	85.2(1)	C(31)–S(3)–N(3)	108.6(2)
S(1)–Zr–S(3)	107.5(1)	N(3)–S(3)–Zr	51.7(1)
S(2)–Zr–Cl	120.5(1)	C(31)–S(3)–Zr	106.6(1)
S(2)–Zr–S(3)	127.5(1)		

Table 4 Selected bond lengths (Å) and angles (°) for $Zr(\eta^2\text{-}Bu^tNSPh)_4$ **4**, with e.s.d.s in parentheses

Zr–N(1)	2.147(4)	S(2)–N(2)	1.690(4)
Zr–N(2)	2.126(4)	S(2)–C(21)	1.797(5)
Zr–N(3)	2.125(4)	S(3)–N(3)	1.688(4)
Zr–N(4)	2.133(4)	S(3)–C(31)	1.796(5)
Zr–S(1)	2.800(1)	S(4)–N(4)	1.686(4)
Zr–S(2)	2.774(2)	S(4)–C(41)	1.798(5)
Zr–S(3)	2.785(2)	N(1)–C(1)	1.507(6)
Zr–S(4)	2.814(1)	N(2)–C(2)	1.501(6)
S(1)–N(1)	1.683(4)	N(3)–C(3)	1.504(5)
S(1)–C(11)	1.802(5)	N(4)–C(4)	1.512(6)
N(1)–Zr–N(2)	132.5(1)	S(2)–Zr–S(4)	102.3(1)
N(1)–Zr–N(3)	99.6(2)	S(3)–Zr–S(4)	79.4(1)
N(1)–Zr–N(4)	101.2(2)	C(1)–N(1)–S(1)	116.1(3)
N(1)–Zr–S(1)	36.9(1)	C(1)–N(1)–Zr	143.4(3)
N(1)–Zr–S(2)	101.6(1)	S(1)–N(1)–Zr	93.2(2)
N(1)–Zr–S(3)	88.0(1)	C(2)–N(2)–S(2)	116.7(3)
N(1)–Zr–S(4)	129.6(1)	C(2)–N(2)–Zr	144.1(3)
N(2)–Zr–N(3)	97.0(1)	S(2)–N(2)–Zr	92.5(2)
N(2)–Zr–N(4)	100.0(2)	C(3)–N(3)–S(3)	117.0(3)
N(2)–Zr–S(1)	99.7(1)	C(3)–N(3)–Zr	143.1(3)
N(2)–Zr–S(2)	37.5(1)	S(3)–N(3)–Zr	93.1(2)
N(2)–Zr–S(3)	128.5(1)	C(4)–N(4)–S(4)	116.1(3)
N(2)–Zr–S(4)	90.7(1)	C(4)–N(4)–Zr	144.5(3)
N(3)–Zr–N(4)	131.8(1)	S(4)–N(4)–Zr	94.2(2)
N(3)–Zr–S(1)	89.6(1)	C(11)–S(1)–N(1)	107.5(2)
N(3)–Zr–S(2)	128.9(1)	N(1)–S(1)–Zr	50.0(1)
N(3)–Zr–S(3)	37.3(1)	C(11)–S(1)–Zr	118.7(2)
N(3)–Zr–S(4)	98.9(1)	C(21)–S(2)–N(2)	107.9(2)
N(4)–Zr–S(1)	130.7(1)	N(2)–S(2)–Zr	50.0(1)
N(4)–Zr–S(2)	88.3(1)	C(21)–S(2)–Zr	119.5(2)
N(4)–Zr–S(3)	100.9(1)	C(31)–S(3)–N(3)	107.9(2)
N(4)–Zr–S(4)	36.7(1)	N(3)–S(3)–Zr	49.6(1)
S(1)–Zr–S(2)	80.8(1)	C(31)–S(3)–Zr	119.1(2)
S(1)–Zr–S(3)	101.2(1)	N(4)–S(4)–C(41)	106.2(2)
S(1)–Zr–S(4)	165.8(1)	N(4)–S(4)–Zr	49.1(1)
S(2)–Zr–S(3)	165.3(1)	C(41)–S(4)–Zr	116.7(2)

group which may ideally be considered to span the 'm' edges. These distortions are represented in Scheme 1.

The 'core tetrahedral' model used for the previous structures

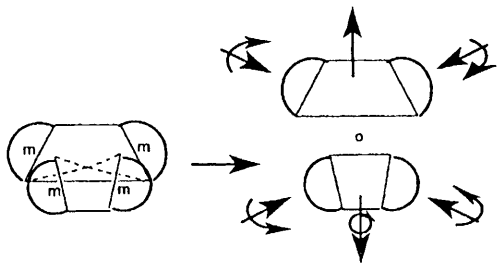

Scheme 1 Distortion of the dodecahedral geometry of complex **4**

may still be used here, even though the ZrN_4 tetrahedron is considerably flattened. This is clearly seen in Fig. 3(*b*) which is a view of the core of the molecule down the bisector of the angles N(2)–Zr–N(3) and N(1)–Zr–N(4). Detailed examination of torsion angles in the structure indicates quite clearly that the S···Zr interactions are directed to faces of the ZrN_4 tetrahedron. In spite of the various distortions, the structure has effective D_2 symmetry and all four ligands are equivalent. However, there is still a small spread in the Zr–N [2.125(4)–2.147(4) Å] and Zr···S distances [2.774(2)–2.814(1) Å], but the N–S distances are all very close [1.683(4)–1.690(4) Å]. The Zr–N distances are similar to those in compound **3**, but the Zr–S are *ca.* 0.1 Å longer.

The ^1H NMR spectrum of complex **4** in $[^2H_8]$tetrahydrofuran is uninformative consisting of a single broad line in the *tert*-butyl region together with complicated aromatic resonances. There is no change over the range −60 to +60 °C; study in toluene is difficult due to low solubility.

The interaction of $ZrCl_2(\eta^5\text{-}C_5H_5)_2$ with 1 or 2 equivalents of $LiN(Bu^t)SPh$ results in formation only of $ZrCl(\eta^5\text{-}C_5H_5)_2(\eta^2\text{-}Bu^tNSPh)$ **5**; no disubstituted species is observed. This contrasts with the situation for α-zirconocenyl thioethers,[13] $ZrCl_n(\eta^5\text{-}C_5H_5)_2(CHPhSPh)_{2-n}$, $n = 0$ or 1, but, like these compounds, **4** shows two sets of C_5H_5 resonances in the ^1H NMR spectrum at *ca.* 25 °C. The ratio of each set of these bands to the two Bu^tN bands (which are in a 1:4 ratio) is *ca.* 1:1. The spectra are thus consistent with the presence in solution of two geometrical isomers in a 1:4 ratio. The magnetic inequivalence of the C_5H_5 rings in each geometrical isomer is expected in view of the presence of two invertomers which are rigid at room temperature. The similar situation for the zirconocenyl thioethers has been considered in detail.[13] The present spectra are unchanged up to +50 °C where the Bu^tN peak of the minor isomer begins to broaden, as occurs also for one set of C_5H_5 bands. Analogous behaviour of the major component starts at +60 °C but at +80 °C both Bu^tN resonances collapse to a broad singlet, while in the C_5H_5 region there are still two bands in a 1:4 ratio. All the changes are reversible and the behaviour can partly be explained by assuming an increased rate of sulfur inversion in each isomer as the temperature increases. It is not obvious why the two Bu^tN peaks also collapse unless it is assumed that the Zr–S bond is broken.

Although there are isomers in solution, attempts to separate *endo* and *exo* isomers by fractional crystallisation were unsuccessful. The crystal structure of the *exo* isomer is shown in Fig. 4(*a*); selected bond lengths and angles are in Table 5. It is possible that only one isomer crystallises under the conditions used or that only an *exo* isomer crystal was selected. The geometry of the molecule is broadly as expected and the origin of the inequivalence of the C_5H_5 rings is seen in Fig. 4(*b*). Whilst the N–S vector lies close to the plane containing the Zr–Cl bond and bisecting the Cp–Zr–Cp angle, the pyramidality of the sulfur destroys the local mirror symmetry. Inversion of the sulfur will lead only to the enantiomeric structure and so the existence of isomers must indeed relate to the orientation of the N–S vector, to give the *endo* and *exo* forms.

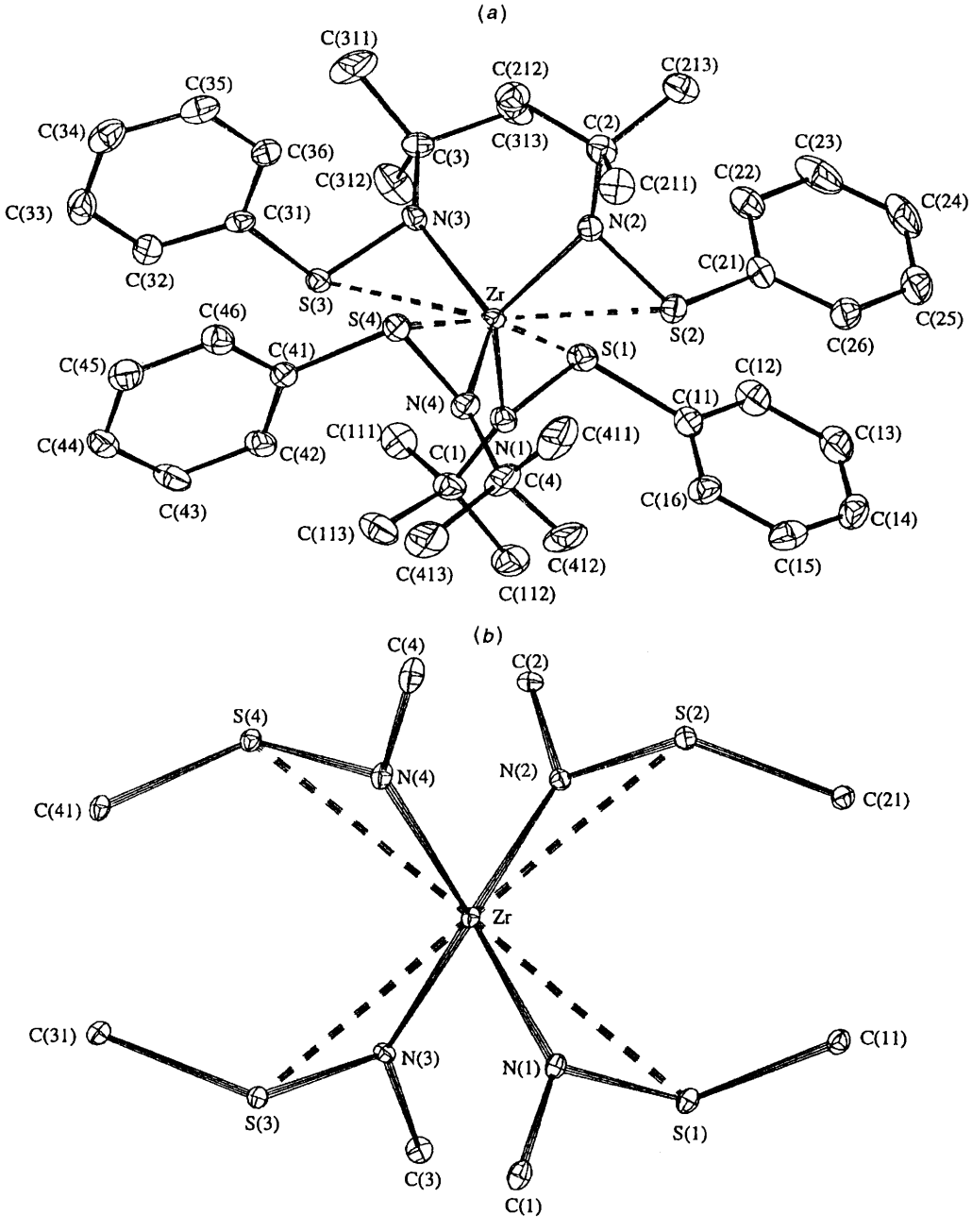

Fig. 3 Structure of $Zr(\eta^2\text{-Bu}^t\text{NSPh})_4$ **4** (*a*) and its core (*b*)

Table 5 Selected bond lengths (Å) and angles (°) for $ZrCl(\eta^5\text{-}C_5H_5)_2(\eta^2\text{-Bu}^t\text{NSPh})$ **5**, with e.s.d.s in parentheses

Zr–N	2.137(8)	Zr–Cp2	2.25(1)
Zr–S	2.681(4)	S–N	1.658(7)
Zr–Cl	2.535(3)	S–C(11)	1.792(9)
Zr–Cp1	2.24(1)	N–C(1)	1.504(10)
N–Zr–Cl	86.9(2)	Cl–Zr–Cp2	100.0(3)
N–Zr–Cp1	115.4(3)	Cp1–Zr–Cp2	126.3(3)
N–Zr–Cp2	113.7(3)	C(1)–N–S	120.3(6)
N–Zr–S	38.2(3)	C(1)–N–Zr	144.1(6)
S–Zr–Cl	124.7(3)	S–N–Zr	88.9(3)
S–Zr–Cp1	107.1(3)	C(11)–S–N	107.7(4)
S–Zr–Cp2	98.1(3)	N–S–Zr	52.9(3)
Cl–Zr–Cp1	102.9(3)	C(11)–S–Zr	121.8(3)

Cp1 is the centroid of the C_5H_5 ring C(21)–C(25), Cp2 that of the ring C(31)–C(35).

The Zr–N and Zr···S distances are similar to those in compound **3**, but the Cl–Zr–N angle, at 86.9(2)° is far from tetrahedral. We presume this distortion is due to the steric crowding present in this structure due to the C_5H_5 co-ordination. We also assume that the preference for this *exo* isomer is linked to minimisation of steric interaction, which will be aided by the long Zr···S bond and distal arrangement of the bulky NBu^t component.

Molybdenum and tungsten complexes

The interaction of $MO_2Cl_2(dme)$ (dme = 1,2-dimethoxyethane) with $LiN(Bu^t)SPh$ in thf at low temperature gives the compounds $MO_2(\eta^2\text{-Bu}^t\text{NSPh})_2$, (M = Mo **6** or W **7**). The addition of the lithium reagent needs care as too rapid addition and temperatures above *ca.* −70 °C produces unidentified reduced species. The structure of **6** determined by X-ray diffraction is shown in Fig. 5; selected bond lengths and angles are in Table 6. Not unexpectedly, this structure is closely analogous to that of the bis(imido)tungsten complex,[6] including the orientation of the N–S vectors and the sulfur lone pairs, which point towards the two faces defined by the two nitrogens and one oxygen. The Mo–O and Mo···S distances

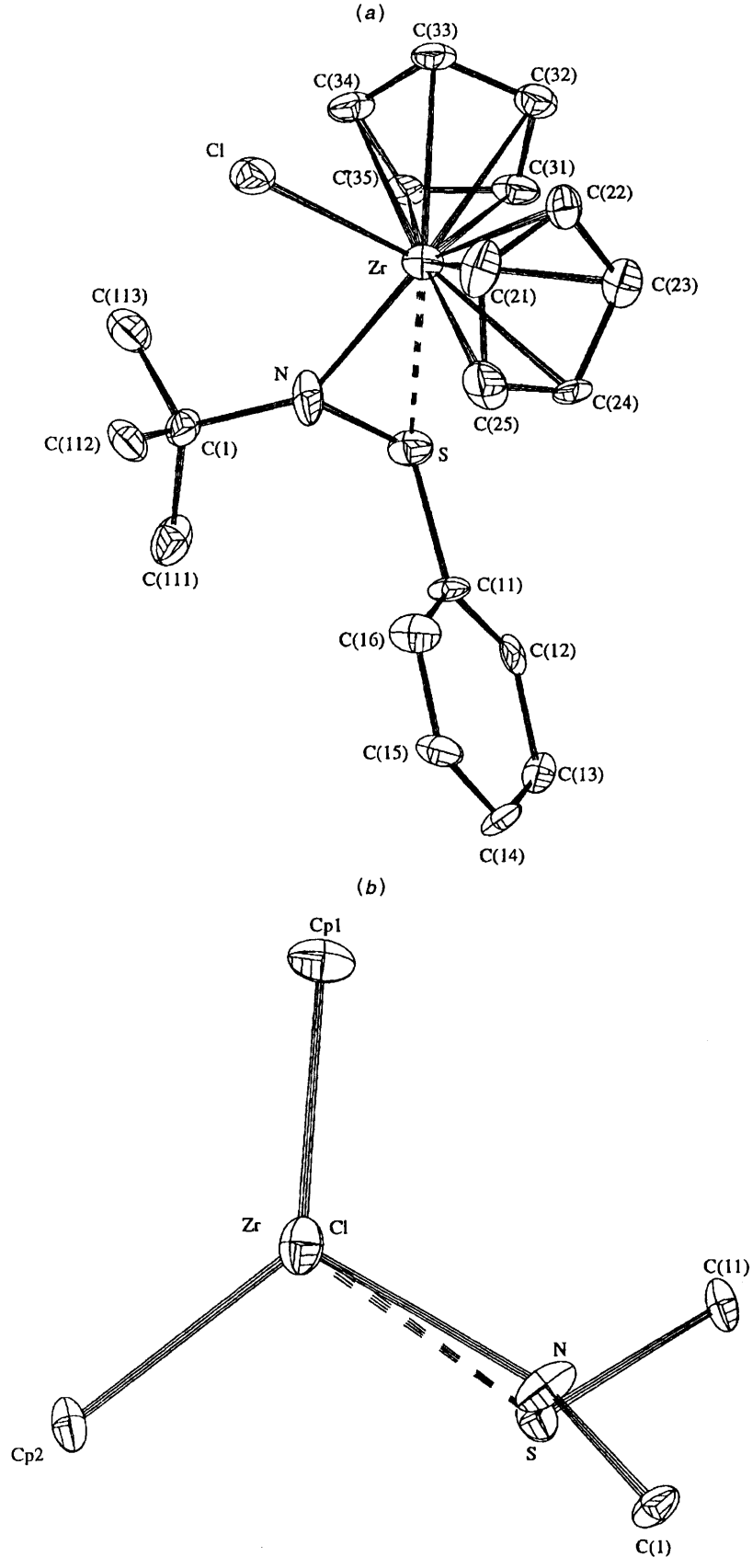

Fig. 4 Structure of the *exo* isomer of $ZrCl(\eta^5\text{-}C_5H_5)_2(\eta^2\text{-}Bu^tNSPh)$ **5** (*a*) and its core viewed along the Cl–Zr bond (*b*); Cpl and Cp2 represent the centroids of the C_5H_5 rings C(21)–C(25) and C(31)–C(35), respectively

are each some 0.05 Å shorter than the analogous bonds in the tungsten complex. The analytical and spectroscopic data for both **6** and **7** are consistent with the structures; the ^1H NMR spectra show Bu^tN and aromatic bands.

Similar compounds can be obtained using $MoCl_2(NBu^t)_2$ or $WCl_2(NBu^t)_2(py)_2$ (py = pyridine) to give the complexes $M(NBu^t)_2(\eta^2\text{-}Bu^tNSPh)_2$ (M = Mo **8** or W **9**) respectively, both of which have identical ^1H NMR spectra as shown by Bu^tN and Bu^tNS peaks and the aromatic peaks. Complex **9** was first made by interaction of $Li_2W(NBu^t)_4$ with PhSCl; the

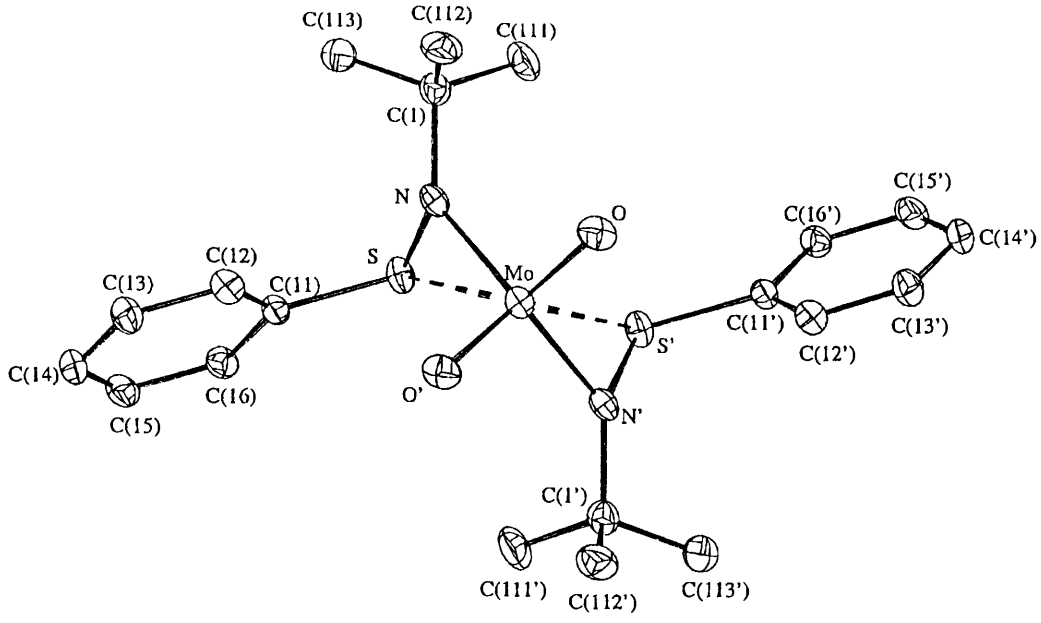

Fig. 5 Structure of $MoO_2(\eta^2\text{-}Bu^tNSPh)_2$ **6**

Table 6 Selected bond lengths (Å) and angles (°) for $MoO_2(\eta^2\text{-}Bu^tNSPh)_2$ **6**, with e.s.d.s in parentheses

Mo–N	1.969(4)	S–N	1.686(4)
Mo–S	2.724(1)	S–C(11)	1.769(5)
Mo–O	1.694(3)	N–C(1)	1.491(6)
O'–Mo–O	109.3(2)	S–Mo–S'	73.6(1)
O'–Mo–N	105.9(2)	N–S–C(11)	104.9(2)
O–Mo–N	104.7(2)	N–S–Mo	45.9(1)
N–Mo–N'	125.8(2)	C(11)–S–Mo	110.9(2)
O'–Mo–S	99.9(1)	C(1)–N–S	120.5(3)
O–Mo–S	139.0(1)	C(1)–N–Mo	135.7(3)
N–Mo–S	38.0(1)	S–N–Mo	96.1(2)
N'–Mo–S	93.3(1)		

Primed atoms are related by the symmetry transformation $-x$, y, $-z + \frac{1}{2}$.

Table 7 Selected bond lengths (Å) and angles (°) for $W(NBu^t)_2(\eta^2\text{-}Bu^tNSePh)_2$ **11**, with e.s.d.s in parentheses

W–N(1)	2.017(6)	Se(1)–C(11)	1.947(8)
W–N(2)	2.008(5)	Se(2)–N(2)	1.842(6)
W–N(3)	1.732(7)	Se(2)–C(21)	1.931(9)
W–N(4)	1.743(6)	N(1)–C(1)	1.507(10)
W–Se(1)	2.941(3)	N(2)–C(2)	1.504(9)
W–Se(2)	2.922(2)	N(3)–C(3)	1.469(10)
Se(1)–N(1)	1.828(7)	N(4)–C(4)	1.463(9)
N(1)–W–N(2)	124.2(2)	C(1)–N(1)–Se(1)	117.6(6)
N(1)–W–N(3)	107.4(3)	C(1)–N(1)–W	135.7(6)
N(1)–W–N(4)	104.5(3)	Se(1)–N(1)–W	99.7(3)
N(1)–W–Se(1)	37.8(2)	C(2)–N(2)–Se(2)	118.5(4)
N(1)–W–Se(2)	92.9(2)	C(2)–N(2)–W	134.1(4)
N(2)–W–N(3)	104.3(3)	Se(2)–N(2)–W	98.7(3)
N(2)–W–N(4)	105.7(2)	C(3)–N(3)–W	164.4(6)
N(2)–W–Se(1)	90.9(2)	C(4)–N(4)–W	160.1(5)
N(2)–W–Se(2)	38.6(2)	C(11)–Se(1)–N(1)	102.5(3)
N(3)–W–N(4)	110.6(3)	N(1)–Se(1)–W	42.5(2)
N(3)–W–Se(1)	139.6(2)	C(11)–Se(1)–W	108.3(3)
N(3)–W–Se(2)	96.3(2)	C(21)–Se(2)–N(2)	102.8(3)
N(4)–W–Se(1)	100.4(2)	N(2)–Se(2)–W	42.8(2)
N(4)–W–Se(2)	141.2(2)	C(21)–Se(2)–W	106.2(3)
Se(1)–W–Se(2)	72.68(8)		

products by both methods are identical according to spectroscopic, analytical and physical data. The structure of **9** was reported[6] and that of **8** is clearly similar.

In the ^1H NMR spectrum of complexes **8** and **9** there appears to be a minor isomer or invertomer in about 5% abundance. On raising the temperature the *tert*-butyl resonances of the two invertomers coalesce to yield two broad peaks (ratio 1 : 1) at *ca.* + 70 °C. At higher temperatures further broadening of the peak assigned as Bu^tNS occurs while that for the Bu^tN group becomes sharp up to 110 °C, the highest temperature suitable for study. Use of $LiN(Bu^t)SC_6H_2Me_3$-2,4,6 with $MoCl_2(N\text{-}Bu^t)_2$ gives only the monosubstituted $MoCl(NBu^t)_2(Bu^tNSC_6\text{-}H_2Me_3\text{-}2,4,6)$ **10** characterised spectroscopically. The selenium analogue of **9**, $W(NBu^t)_2(\eta^2\text{-}Bu^tNSePh)_2$ **11** was made by the same route, namely the interaction of $Li_2W(NBu^t)_4$ and PhSeBr, as colourless crystals.

The structure of complex **11** is shown in Fig. 6 and bond parameters are given in Table 7. This complex is actually isostructural with the sulfur analogue previously reported.[6] The W–N (amido) bond lengths are very similar between the two, but the W–N (imido) lengths are slightly shorter here than in the sulfur complex. The W···Se and Se–N distances are both some 0.15 Å longer than distances involving sulfur.

The ^1H NMR spectrum of complex **11** shows one sharp and one broad peak for the *tert*-butyl group at *ca.* 25 °C in $[^2H_8]$toluene; the sharp peak is assigned to the Bu^tN imido group. The spectrum corresponds to that observed for the sulfur analogues **8** and **9** above + 100 °C. On heating both peaks sharpen at *ca.* 50 °C and remain so to 100 °C. On cooling to *ca.* − 10 °C the *tert*-butylimido bands split into two of equal intensity (− 20 °C) while at − 30 °C the *tert*-butylamido peak is split into two. There is no change in the spectra at lower temperatures. This behaviour can be rationalised by assuming that the selenium inversion becomes slower giving rise to invertomers having magnetically inequivalent *tert*-butyl-imido and -amido groups [*cf.* $ZrCl(\eta^5\text{-}C_5H_5)_2(\eta^2\text{-}Bu^tNSPh)$]. These observations suggest that there is a higher activation energy for the sulfenamido inversion than for the selenium one; this differs from the scarce data available for thio- and seleno-ethers,[11] but of course the compounds are quite different in structure. An additional factor that should affect the inversion is the rotation barrier around the nitrogen–chalcogen bond which probably accompanies the inversion process. In the sulfur compound this is expected to be higher than in the selenium one, accounting for the higher total activation energy.

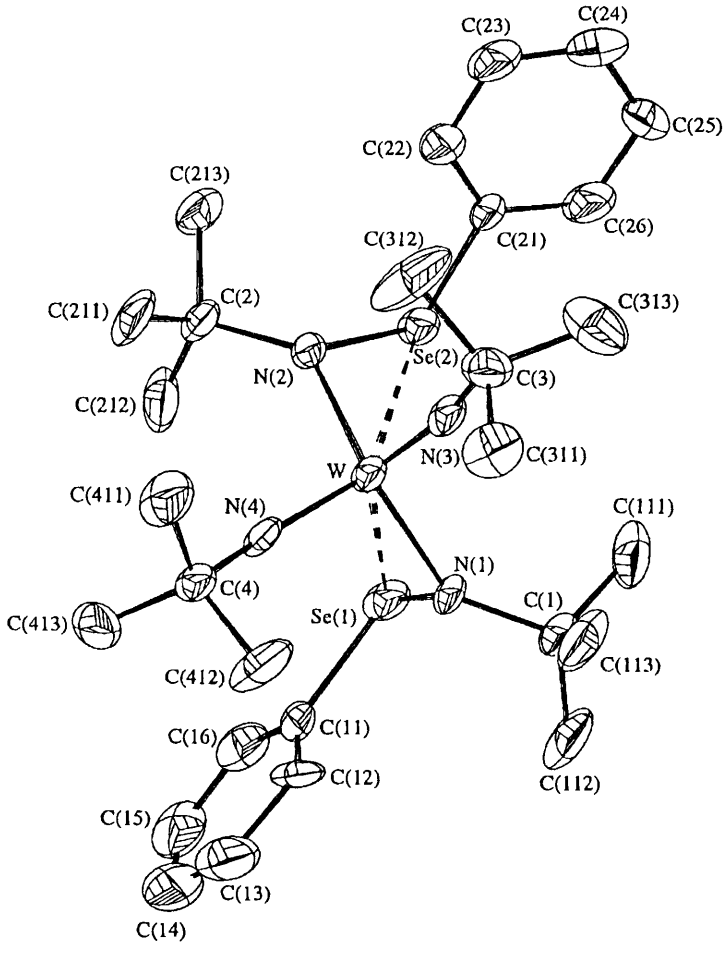

Fig. 6 Structure of $W(NBu^t)_2(\eta^2\text{-}Bu^tNSePh)_2$ **11**

Experimental

Analyses were by the Imperial College microanalytical laboratory. All operations were carried out under purified N_2 or Ar, under vacuum or in a Vacuum Atmospheres box. General techniques and instrumentation used have been described.[14] Proton NMR data were obtained on a JEOL EX-270 spectrometer operating at 270 MHz (^1H) and referenced to residual H impurity in the solvent (δ 7.15, C_6D_6), selenium NMR data on a JEOL FX-90Q spectrometer operating at 17.01 MHz and referenced to external Me_2Se (δ 0.0). Mass spectra were obtained on VG-7070E (EI) and Autospec (GC-MS and FAB) instruments. Calculated isotopic envelopes were in good agreement with experimental patterns.

Commercial chemicals were from Aldrich, Avocado and Fluka; the light petroleum used had b.p. 40–60 °C. Literature procedures were used for $Li_2W(NBu^t)_4$,[15] $ZrCl_4(tht)_2$,[16] $MoO_2Cl_2(dme)$,[17] $WO_2Cl_2(dme)$,[18] $MoCl_2(NBu^t)_2$,[19] $WCl_2(NBu^t)_2(py)_2$,[20] PhSCl[21a] and PhSeBr.[21b]

The main starting material, $Bu^tN(H)SPh$,[8] is readily made in up to *ca.* 100 g quantities as follows. To NH_2Bu^t (16 g, 0.22 mol) in Et_2O (300 cm^3) at −40 °C was added PhSCl (14.5 g, 0.1 mol) in Et_2O (100 cm^3) dropwise (using mechanical stirring in a larger-scale synthesis). After stirring for 30 min the solution was allowed to warm to room temperature; filtration and removal of Et_2O under vacuum left a product that was purified by vacuum distillation [*ca.* 60 °C, 0.08 mmHg (*ca.* 10.6 Pa)].

The synthesis of PhN(H)SPh is typical for that of other arylamido compounds. To NH_2Ph (20.5 g, 0.22 mol) in Et_2O (300 cm^3) at −78 °C was added PhSCl (14.5 g, 0.1 mol) in Et_2O (100 cm^3) slowly with stirring. After warming to room temperature and stirring for *ca.* 2 h, removal of ether under vacuum, extraction of the residue with light petroleum followed by filtration and removal of solvent under vacuum left the crude product. Repeated crystallisation (usually three times) from light petroleum gave a colourless crystalline solid; the final crystallisation was made under N_2 at −20 °C. Yield *ca.* 70%, m.p. 56–58 °C. Other compounds have been made similarly using NH_2R (R = C_6H_4Me-*p* or -*o*, or $C_6H_4Pr^i$-*o*). As noted earlier, the best yields are obtained under dry air or oxygen.

The compound $Bu^tN(H)SC_6H_2Me_3$-2,4,6 was obtained as follows: to NH_2Bu^t (8 g, 0.11 mol) in Et_2O (100 cm^3) at −78 °C was added 2,4,6-$Me_3C_6H_2SCl$[22] (9.3 g, 0.05 mol) in Et_2O (50 cm^3). After reaching room temperature the mixture was stirred for 1 h when solvent was removed under vacuum. The residue was extracted with light petroleum which was filtered and evaporated. The product was used without further purification. Yield *ca.* 80%, m.p. *ca.* 30 °C.

The selenium analogue $Bu^tN(H)SeC_6H_2Me_3$-2,4,6 was made as follows: to NH_2Bu^t (1.3 g, 5 equivalents) at −78 °C was added, under N_2 and dropwise, a solution of 2,4,6-$Me_3C_6H_2SeBr$ (1 g, 1 equivalent) in Et_2O (40 cm^3). After the addition the white suspension was allowed to reach room temperature (*ca.* 3 h) and stirred (5 h). Filtration under N_2 and removal of volatiles under vacuum left $Bu^tN(H)SeC_6H_2Me_3$-2,4,6 (> 90% pure according to ^{77}Se NMR spectroscopy) as a yellow oil in *ca.* 75% yield. NMR (C_6D_6): ^1H, δ 6.8 (s, 2 H, aromatic), 2.8 (s, br, 1 H, N*H*Bu^t), 2.7 (s, 6 H, *o*-Me of $C_6H_2Me_3$), 2.2 (s, 3 H, *p*-Me of $C_6H_2Me_3$) and 1.1 (s, 9 H, $NCMe_3$); ^{77}Se, δ 518.

Preparation of complexes

Bis(*N-tert*-butylbenzenesulfenamido)dichlorotitanium(IV) 1. To a solution of $TiCl_4$ (0.19 g, 1 mmol) in toluene (30 cm^3) at −78 °C was added dropwise a suspension of LiN(Bu^t)SPh

Table 8 Crystal data and structure refinement details for compounds **1**, **3**–**6** and **11**

	1	**3**	**4**	**5**	**6**	**11**
Formula	$C_{20}H_{28}Cl_2N_2S_2Ti$	$C_{30}H_{42}ClN_3S_3Zr$	$C_{40}H_{56}N_4S_4Zr$	$C_{20}H_{24}ClNSZr$	$C_{20}H_{28}MoN_2O_2S_2$	$C_{28}H_{46}N_4Se_2W$
M_r	479.36	667.52	812.35	437.13	488.5	780.46
Crystal system	Triclinic	Monoclinic	Monoclinic	Orthorhombic	Monoclinic	Triclinic
Space group	$P\bar{1}$	$P2_1/c$	$P2_1/n$	$P2_12_12_1$	$C2/c$	$P\bar{1}$
a/Å	8.844(8)	15.217(5)	11.287(6)	7.722(1)	22.584(2)	10.637(8)
b/Å	11.736(7)	12.173(6)	22.824(7)	14.982(3)	6.068(2)	11.19(1)
c/Å	12.244(5)	18.436(4)	19.207(8)	16.570(6)	15.895(3)	16.411(7)
α/°	76.20(3)					102.78(9)
β/°	76.58(3)	106.68(3)	104.22(2)		98.12(1)	97.19(9)
γ/°	73.97(2)					117.68(4)
U/Å^3	1167(1)	3271(2)	4796(4)	1917(1)	2156(1)	1627(2)
Z	2	4	4	4	4	2
D_c/Mg m^{-3}	1.364	1.355	1.125	1.515	1.505	1.593
F(000)	500	1392	1712	896	1008	768
Crystal size/mm	0.25 × 0.20 × 0.10	0.24 × 0.17 × 0.15	0.48 × 0.36 × 0.18	0.18 × 0.07 × 0.07	0.70 × 0.05 × 0.05	0.15 × 0.10 × 0.09
μ(Mo-Kα)/mm^{-1}	0.782	0.605	0.412	0.823	0.819	5.669
Collection temperature/K	140	150	150	120	150	293
Reflections collected	3901	13 316	15 747	7851	3757	6880
Independent reflections (R_{int})	3057 (0.0666)	4837 (0.0562)	7138 (0.0413)	2983 (0.0931)	1663 (0.0471)	4560 (0.0405)
Maximum, minimum correction factors	—, —	1.046, 0.900	1.090, 0.816	1.124, 0.879	1.054, 0.883	1.152, 0.883
Data, restraints, parameters	3057, 0, 250	4834, 0, 412	7110, 0, 454	2981, 0, 220	1663, 0, 126	4558, 0, 328
Goodness of fit, F^2	0.444	0.809	1.063	0.719	0.426	0.817
Final $R1$, $wR2$						
$[I > 2\sigma(I)]$	0.0545, 0.1254	0.0360, 0.0684	0.0620, 0.1880	0.0492, 0.0809	0.0306, 0.0792	0.0350, 0.066
(all data)	0.1296, 0.2203	0.0715, 0.0737	0.0712, 0.2204	0.0991, 0.0987	0.0504, 0.1021	0.0510, 0.068
Largest difference peak and hole/e Å^{-3}	0.717, −0.266	0.583, −0.323	1.805, −0.683	1.152, −0.479	0.408, −0.378	1.312, −0.825

$S = [\Sigma w(F_o^2 - F_c^2)^2/(n-p)]^{\frac{1}{2}}$, $R_1 = \Sigma||F_o| - |F_c||/\Sigma|F_o|$, $wR2 = [\Sigma w(F_o^2 - F_c^2)^2/\Sigma w(F_o^2)^2]^{\frac{1}{2}}$, $w = 1/[\sigma^2(F_o^2) + (xP)^2 + gP]$, $P = [\max(F_o^2) + 2F_c^2]/3$, where n = number of reflections and p = total number of parameters, x = 0.0000, 0.0159, 0.1341, 0.0000, 0.0000 and 0.0147 and g = 0, 0, 6.83, 0, 0 and 0 for compounds **1**, **3**, **4**, **5**, **6** and **11** respectively.

(0.39 g, 2.1 mmol) in toluene (30 cm^3). After reaching room temperature the mixture was stirred for 12 h. Removal of volatiles under vacuum, extraction of the residue into light petroleum (3 × 20 cm^3) followed by filtration, concentration to *ca.* 30 cm^3 and cooling to −20 °C gave lemon-yellow crystals. Yield: 0.26 g, 67%. Mass spectrum (EI): *m/z* 478 (M^+), 422 ($M^+ - Me_2C{=}CH_2$) and 366 ($M^+ - 2Me_2C{=}CH_2$). NMR (C_6D_6): ^1H, δ 1.30 (s, 18 H, Me_3CNS), 1.34 (s, 18 H, Me_3CNS) and 6.9–7.5 (m, 20 H, Ph).

Bis(*N-tert*-butyl-2,4,6-trimethylbenzenesulfenamido)-dichlorotitanium(IV) 2. This complex was made as for **1** from $TiCl_4$ (0.19 g, 1 mmol) and $LiN(Bu^t)SC_6H_2Me_3$-2,4,6 (0.48 g, 2.1 mmol). Yield: 0.21 g, 37%. NMR (C_6D_6): ^1H, δ 1.37 (s, 18 H, Me_3CNS), 1.96 (s, 6 H, *p*-Me of $C_6H_2\mathit{Me}_3$), 2.66 (s, 12 H, *o*-Me of $C_6H_2\mathit{Me}_3$) and 6.54 (s, 4 H, $SC_6\mathit{H}_2Me_3$).

Tris(*N-tert*-butylbenzenesulfenamido)chlorozirconium(IV) 3. To a suspension of $ZrCl_4$ (0.23 g, 1 mmol) in toluene (30 cm^3) at −78 °C was added dropwise a suspension of $LiN(Bu^t)SPh$ (0.58 g, 3.1 mmol). The mixture was allowed to reach room temperature and stirred for 12 h. Removal of volatiles under vacuum, extraction of the residue with light petroleum (3 × 20 cm^3) followed by filtration through a Celite pad, concentration to *ca.* 30 cm^3 and cooling to −20 °C gave colourless crystals. Yield: 0.18 g, 27%. Mass spectrum (EI): *m/z* 667 (M^+), 611 ($M^+ - Me_2C{=}CH_2$) and 487 ($M^+ - Bu^tNSPh$). NMR (C_6D_6): ^1H, δ 1.0, 1.35, 1.48, 1.50 (s, 9 H, Me_3CNS; peaks are in 1:1:1:1 ratio due to the presence of isomers) and 6.88–7.50 (m, 5 H, Ph).

Tetrakis(*N-tert*-butylbenzenesulfenamido)zirconium(IV) 4. To a suspension of $ZrCl_4(tht)_2$ (0.41 g, 1 mmol) in toluene (30 cm^3) at room temperature was added dropwise a suspension of $LiN(Bu^t)SPh$ (0.97 g, 5.2 mmol). The mixture was stirred for 12 h, filtered through a Celite pad and concentrated to *ca.* 15 cm^3. The product was obtained either as colourless crystals by cooling to −20 °C or as a powder by precipitation with light petroleum. Yield: 0.39 g, 48%. NMR (C_4D_8O): ^1H, δ 1.22 (s, 36 H, Me_3CNS) and 7.04–7.39 (m, 20 H, Ph).

Table 9 Fractional atomic coordinates (× 10^4) for compound **1**

Atom	*x*	*y*	*z*
Ti	3629(2)	6907(1)	2248(1)
Cl(1)	1267(3)	6632(2)	2003(2)
Cl(2)	4938(3)	4958(2)	2758(2)
S(1)	3836(3)	8638(2)	618(2)
S(2)	2052(3)	8458(2)	3464(2)
N(1)	5040(9)	7238(6)	843(6)
N(2)	3918(9)	7590(6)	3422(6)
C(1)	6686(11)	6922(7)	121(8)
C(2)	5060(12)	7859(8)	4009(8)
C(11)	2736(11)	8652(8)	−420(8)
C(12)	2785(12)	7663(8)	−867(9)
C(13)	1922(13)	7761(9)	−1707(8)
C(14)	966(13)	8880(9)	−2110(9)
C(15)	889(12)	9879(9)	−1688(9)
C(16)	1764(12)	9772(8)	−865(8)
C(21)	797(11)	7736(8)	4646(7)
C(22)	−612(12)	8455(9)	5115(8)
C(23)	−1628(11)	7929(9)	6012(8)
C(24)	−1227(14)	6710(9)	6433(9)
C(25)	220(15)	5996(9)	5961(9)
C(26)	1242(13)	6543(8)	5085(8)
C(111)	6930(13)	7891(9)	−940(8)
C(112)	6867(13)	5721(8)	−234(10)
C(113)	7940(12)	6750(10)	864(9)
C(211)	4226(13)	8075(10)	5219(9)
C(212)	6476(11)	6785(10)	4051(9)
C(213)	5518(14)	8980(10)	3333(10)

(*N-tert*-butylbenzenesulfenamido)chlorobis(η⁵-cyclopentadienyl)zirconium(IV) 5. To a solution of $ZrCl_2(\eta^5\text{-}C_5H_5)_2$ (0.29 g, 1 mmol) in toluene (30 cm^3) at −78 °C was added dropwise a suspension of $LiN(Bu^t)SPh$ (0.21 g, 1.1 mmol). The mixture was then allowed to reach room temperature and stirred for 12 h. Removal of solvent under vacuum, extraction of the residue with light petroleum (3 × 20 cm^3), followed by filtration, concentration to *ca.* 30 cm^3, and cooling at −20 °C gave pale yellow crystals. Yield: 0.29 g, 67%. Mass spectrum (EI): *m/z* 435 (M^+), 379 ($M^+ - Me_2C{=}CH_2$), 370 ($M^+ - C_5H_5$), and 255 ($M^+ - Bu^tNSPh$). NMR (C_6D_6): ^1H, δ 1.52 (s, 9 H, Me_3CNS), 5.68 (s, 5 H, C_5H_5), 5.90 (s, 5 H, C_5H_5) and 6.91–7.25 (m, 5 H, Ph).

Bis(*N-tert*-butylbenzenesulfenamido)dioxomolybdenum(VI) 6. To a solution of MoO_2Cl_2(dme) (0.29 g, 1 mmol) in thf (30 cm^3) at −78 °C was added dropwise a solution of $LiN(Bu^t)SPh$ (0.39 g, 2.1 mmol) in thf (20 cm^3). The mixture was allowed to reach room temperature and stirred for 12 h. The volatiles were removed under vacuum and the residue was washed with light petroleum. Extraction into toluene (2 × 20 cm^3) followed by filtration, concentration to *ca.* 30 cm^3 and cooling to −20 °C gave pale green crystals. Yield: 0.22 g, 46%. Mass spectrum (EI): *m/z* 490 (M^+), 434 ($M^+ - Me_2C{=}CH_2$), 378 ($M^+ - 2Me_2C{=}CH_2$) and 310 ($M^+ - Bu^tNSPh$). NMR (C_6D_6): ^1H, δ 1.29 (s, 18 H, Me_3CNS) and 6.87–7.40 (m, 10 H, Ph).

Bis(*N-tert*-butylbenzenesulfenamido)dioxotungsten(VI) 7. As for complex **6** but using WO_2Cl_2(dme) (0.38 g, 1 mmol) and $LiN(Bu^t)SPh$ (0.39 g, 2.1 mmol) to give pale yellow crystals. Yield: 0.25 g, 44%. Mass spectrum (EI): *m/z* 576 (M^+), 520

Table 10 Fractional atomic coordinates (× 10^4) for compound **3**

Atom	*x*	*y*	*z*
Zr	2 738(1)	1 980(1)	8 749(1)
Cl	4 018(1)	2 446(1)	9 863(1)
S(1)	2 471(1)	854(1)	7 451(1)
S(2)	1 306(1)	868(1)	8 903(1)
S(3)	2 811(1)	4 135(1)	8 419(1)
N(1)	3 409(2)	1 550(3)	7 946(2)
N(2)	2 402(2)	658(3)	9 358(2)
N(3)	1 873(2)	3 310(3)	8 255(2)
C(1)	4 090(3)	1 906(4)	7 534(2)
C(2)	2 659(3)	−351(4)	9 854(2)
C(3)	1 019(3)	3 708(4)	7 686(2)
C(11)	2 715(3)	−578(3)	7 618(2)
C(12)	3 531(4)	−963(4)	8 101(3)
C(13)	3 689(3)	−2 064(5)	8 213(3)
C(14)	3 034(5)	−2 805(5)	7 841(3)
C(15)	2 219(4)	−2 437(5)	7 358(3)
C(16)	2 065(4)	−1 324(4)	7 245(3)
C(21)	822(3)	1 732(3)	9 484(2)
C(22)	1 361(4)	2 366(4)	10 070(2)
C(23)	933(4)	3 053(5)	10 458(3)
C(24)	−19(4)	3 151(4)	10 261(3)
C(25)	−531(4)	2 494(5)	9 689(3)
C(26)	−127(3)	1 788(4)	9 294(3)
C(31)	2 931(3)	4 874(4)	9 288(2)
C(32)	3 724(4)	5 479(4)	9 552(3)
C(33)	3 882(4)	6 072(4)	10 215(3)
C(34)	3 248(4)	6 028(4)	10 624(3)
C(35)	2 467(4)	5 426(4)	10 351(3)
C(36)	2 299(4)	4 839(4)	9 676(2)
C(111)	4 840(3)	2 524(4)	8 114(2)
C(112)	3 616(3)	2 674(4)	6 878(2)
C(113)	4 494(3)	918(4)	7 235(2)
C(211)	2 333(3)	−179(4)	10 574(2)
C(212)	2 209(3)	−1 376(4)	9 440(2)
C(213)	3 698(3)	−430(4)	10 090(2)
C(311)	599(3)	4 672(4)	8 003(2)
C(312)	341(3)	2 773(4)	7 509(2)
C(313)	1 220(3)	4 068(4)	6 959(2)

Table 11 Fractional atomic coordinates (× 10^4) for compound **4**

Atom	*x*	*y*	*z*	Atom	*x*	*y*	*z*
Zr	−75(1)	2136(1)	2722(1)	C(31)	−1868(4)	3308(2)	1319(2)
S(1)	703(1)	1050(1)	2321(1)	C(32)	−3028(4)	3438(2)	903(2)
S(2)	1783(1)	1905(1)	3935(1)	C(33)	−3392(5)	4021(2)	799(3)
S(3)	−1482(1)	2544(1)	1413(1)	C(34)	−2603(5)	4469(2)	1100(3)
S(4)	−1337(1)	3061(1)	3190(1)	C(35)	−1448(5)	4334(2)	1510(3)
N(1)	−691(3)	1268(2)	2384(2)	C(36)	−1084(4)	3748(2)	1625(2)
N(2)	1619(3)	2465(2)	3343(2)	C(41)	−2892(4)	3178(2)	2697(2)
N(3)	50(3)	2491(2)	1720(2)	C(42)	−3638(4)	2716(2)	2387(3)
N(4)	−1229(4)	2346(2)	3415(2)	C(43)	−4820(4)	2817(2)	2015(3)
C(1)	−1759(4)	925(2)	1947(3)	C(44)	−5287(4)	3388(2)	1938(3)
C(2)	2323(4)	3014(2)	3599(3)	C(45)	−4551(5)	3855(2)	2252(3)
C(3)	791(4)	2472(2)	1168(2)	C(46)	−3340(4)	3750(2)	2635(3)
C(4)	−1550(5)	2188(2)	4111(3)	C(111)	−1794(5)	929(2)	1148(3)
C(11)	1235(4)	505(2)	3006(3)	C(112)	−1718(5)	292(2)	2199(3)
C(12)	2179(5)	146(2)	2914(3)	C(113)	−2919(5)	1219(3)	2052(3)
C(13)	2636(5)	−277(2)	3441(3)	C(211)	2055(5)	3230(2)	4309(3)
C(14)	2161(5)	−345(2)	4025(3)	C(212)	1873(5)	3480(2)	3028(3)
C(15)	1211(5)	9(2)	4101(3)	C(213)	3693(5)	2926(2)	3701(3)
C(16)	745(5)	440(2)	3596(3)	C(311)	770(6)	3081(3)	813(3)
C(21)	3080(4)	1479(2)	3851(3)	C(312)	324(5)	1999(3)	605(3)
C(22)	3602(4)	1529(2)	3272(3)	C(313)	2089(4)	2314(3)	1551(3)
C(23)	4642(5)	1213(3)	3265(4)	C(411)	−723(6)	2519(3)	4734(3)
C(24)	5149(5)	845(3)	3829(4)	C(412)	−1330(6)	1527(3)	4212(3)
C(25)	4621(5)	787(2)	4400(4)	C(413)	−2888(6)	2320(3)	4074(3)
C(26)	3591(5)	1104(2)	4420(3)				

Table 12 Fractional atomic coordinates (× 10^4) for compound **5**

Atom	*x*	*y*	*z*
Zr	8 761(1)	1 699(1)	1 705(1)
S	9 271(3)	653(2)	2 997(2)
Cl	5 828(3)	2 032(2)	1 088(1)
N	7 392(9)	1 023(5)	2 645(5)
C(11)	9 562(12)	1 110(6)	3 987(5)
C(12)	10 850(12)	738(6)	4 448(5)
C(13)	11 066(14)	1 012(6)	5 260(5)
C(14)	10 001(10)	1 653(7)	5 584(5)
C(15)	8 769(14)	1 991(6)	5 100(5)
C(16)	8 561(12)	1 743(7)	4 296(5)
C(1)	5 738(12)	543(6)	2 849(5)
C(111)	5 918(13)	14(6)	3 634(5)
C(112)	4 368(11)	1 232(6)	2 938(6)
C(113)	5 352(11)	−97(6)	2 178(5)
C(21)	8 506(11)	3 381(6)	1 754(6)
C(22)	9 968(11)	3 212(6)	1 318(5)
C(23)	11 184(13)	2 797(5)	1 859(5)
C(24)	10 402(11)	2 759(6)	2 612(5)
C(25)	8 756(14)	3 118(6)	2 564(6)
C(31)	11 001(14)	667(6)	1 194(5)
C(32)	10 860(13)	1 324(6)	579(5)
C(33)	9 288(13)	1 227(7)	264(5)
C(34)	8 477(14)	500(6)	615(5)
C(35)	9 590(12)	144(6)	1 189(5)

Table 13 Fractional atomic coordinates (× 10^4) for compound **6**

Atom	*x*	*y*	*z*
Mo	0	520(1)	2500
S	−724(1)	−3075(2)	2480(1)
O	305(2)	2136(5)	1805(2)
N	−676(2)	−959(6)	1806(2)
C(11)	−1362(2)	−2483(8)	2972(3)
C(12)	−1671(2)	−482(7)	2862(3)
C(13)	−2162(2)	−156(8)	3262(3)
C(14)	−2357(2)	−1778(8)	3770(3)
C(15)	−2039(2)	−3747(9)	3882(3)
C(16)	−1554(2)	−4126(8)	3489(3)
C(1)	−888(2)	−1213(8)	879(3)
C(111)	−446(2)	−2627(9)	486(3)
C(112)	−938(3)	1051(9)	505(3)
C(113)	−1502(2)	−2288(9)	745(3)

(M^+ − $Me_2C{=}CH_2$), 464 (M^+ − $2Me_2C{=}CH_2$) and 396 (M^+ − Bu^tNSPh). NMR (C_6D_6): ^1H, δ 1.30 (s, 18 H, Me_3CNS) and 6.85–7.51 (m, 10 H, Ph).

Bis(*N-tert*-butylbenzenesulfenamido)bis(*tert*-butylimido)-molybdenum(VI) 8. To a solution of $MoCl_2(NBu^t)_2$ (0.31 g, 1 mmol) in Et_2O (30 cm^3) at −78 °C was added dropwise with stirring a solution of $LiN(Bu^t)SPh$ (0.39 g, 2.1 mmol) in Et_2O (30 cm^3). The mixture was allowed to reach room temperature, stirred for 12 h and volatiles removed under vacuum. Extraction of the residue with light petroleum (3 × 20 cm^3) followed by filtration, concentration to *ca.* 30 cm^3 and cooling to −20 °C gave pale yellow crystals. Yield: 0.38 g, 63%. Mass spectrum (EI): *m/z* 600 (M^+), 544 (M^+ − $Me_2C{=}CH_2$) and 420 (M^+ − Bu^tNSPh). NMR (C_6D_6): ^1H, δ 1.21 (s, 18 H, Me_3CNS), 1.47 (s, 18 H, Me_3CNS) and 7.09–7.37 (m, 10 H, Ph).

Bis(*N-tert*-butylbenzenesulfenamido)bis(*tert*-butylimido)-tungsten(VI) 9. As for complex **8** using $WCl_2(NBu^t)_2(py)_2$ (0.56 g, 1 mmol) and $LiN(Bu^t)SPh$ (0.39 g, 2.1 mmol) to give colourless crystals. Yield: 0.32 g, 46%; m.p. 185–187 °C. Mass spectrum (EI): *m/z* 686 (M^+), 671 (M^+ − Me), 630 (M^+ − $Me_2C{=}CH_2$) and 615 (M^+ − Bu^tN). NMR (C_6D_6): ^1H, δ 1.27 (s, 18 H, Me_3CNS), 1.48 (s, 18 H, Me_3CN) and 6.93–7.37 (m, 10 H, Ph). The analytical and spectroscopic data were the same as those for **9** made by interaction of $Li_2W(NBu^t)_4$ with PhSCl.[6]

(*N-tert*-Butyl-2,4,6-trimethylbenzenesulfenamido)bis(*tert*-butylimido)chloromolybdenum(VI) 10. As for complex **8** using $MoCl_2(NBu^t)_2$ (0.31 g, 1 mmol) and $LiN(Bu^t)SC_6H_2Me_3$-2,4,6 (0.48 g, 2.1 mmol) to give green crystals. Yield: 0.28 g, 56%. Mass spectrum (EI): *m/z* 497 (M^+), 441 (M^+ − $Me_2C{=}CH_2$) and 275 (M^+ − $Bu^tNSC_6H_2Me_3$-2,4,6). NMR (C_6D_6): ^1H, δ 1.27 (s, 9 H, Me_3CNS), 1.45 (s, 18 H, Me_3CN), 2.03 (s, 3 H, *p*-Me of $C_6H_2Me_3$), 2.59 (s, 6 H, *o*-Me of $C_6H_2Me_3$) and 6.57 (s, 2 H, $SC_6H_2Me_3$).

Bis(*N-tert*-butylbenzeneselenamido)bis(*tert*-butylimido)tungsten(VI) 11. To a suspension of $Li_2W(NBu^t)_4$ (0.48 g, 1 mmol) in light petroleum (20 cm^3) at −78 °C was added dropwise a solution of PhSeBr (0.47 g, 2 mmol) in toluene–light petroleum (50:50, 40 cm^3) cooled to −78 °C. The mixture was allowed to reach room temperature slowly and stirred for 12 h. Removal of

Table 14 Fractional atomic coordinates (× 10^4) for compound **11**

Atom	*x*	*y*	*z*
W	154(1)	1501(1)	2575(1)
Se(1)	172(1)	−1061(1)	1652(1)
Se(2)	654(1)	1747(1)	894(1)
N(1)	1230(7)	430(7)	2657(4)
N(2)	−787(6)	1561(6)	1457(3)
N(3)	1380(7)	3272(7)	3166(3)
N(4)	−1264(7)	761(7)	3063(3)
C(11)	−1050(9)	−2607(9)	2064(6)
C(12)	−937(10)	−2325(10)	2938(6)
C(13)	−1932(13)	−3567(14)	3128(7)
C(14)	−2818(15)	−4891(15)	2514(11)
C(15)	−2831(13)	−5026(12)	1673(9)
C(16)	−1927(11)	−3899(11)	1433(7)
C(21)	1714(9)	3759(9)	1043(5)
C(22)	1129(11)	4591(10)	1154(5)
C(23)	1927(12)	6014(11)	1223(6)
C(24)	3343(14)	6605(12)	1170(7)
C(25)	3956(12)	5760(11)	1062(6)
C(26)	3114(12)	4291(11)	984(6)
C(1)	2792(10)	826(10)	3027(6)
C(111)	3746(10)	1586(13)	2483(6)
C(112)	2876(11)	−451(11)	3081(6)
C(113)	3277(10)	1869(11)	3934(6)
C(2)	−2349(9)	852(9)	923(4)
C(211)	−3176(9)	1239(10)	1514(5)
C(212)	−3002(9)	−747(10)	563(6)
C(213)	−2429(10)	1473(11)	179(5)
C(3)	2076(11)	4734(10)	3756(5)
C(311)	2264(10)	4760(9)	4704(5)
C(312)	1027(13)	5292(11)	3546(6)
C(313)	3582(11)	5611(11)	3618(6)
C(4)	−2096(9)	595(9)	3716(5)
C(411)	−2410(11)	1821(10)	3977(5)
C(412)	−1102(11)	701(11)	4514(5)
C(413)	−3544(10)	−833(10)	3348(6)

volatiles under vacuum, extraction of the residue with light petroleum (3 × 20 cm^3) followed by filtration, concentration to *ca.* 30 cm^3 and cooling to −20 °C gave colourless crystals. Yield: 0.74 g, 95%. Mass spectrum (EI): *m/z* 780 (M^+), 765 (M^+ − Me), 724 (M^+ − $Me_2C{=}CH_2$) and 709 (M^+ − Bu^{t}N). NMR (C_6D_6): ^{1}H, δ 1.36 (s, 18 H, $SeNCMe_3$), 1.48 (s, 18 H, Me_3CN) and 6.95–7.47 (m, 10 H, Ph).

X-Ray crystallography

X-Ray data for compounds **1** and **3**–**6** were collected at low temperature, those for **11** at room temperature (see Table 8). A FAST TV area-detector diffractometer with Mo-Kα radiation (λ = 0.710 69 Å) was employed, as previously described.[23] Compounds **5**, **6** and **11** were solved using the PATT instruction of SHELXS 86,[24] **1**, **3** and **4** *via* direct methods of the same program. The structures were refined by full-matrix least squares on F_o^2, using the program SHELXL 93.[25] All unique data used were corrected for Lorentz and polarisation factors. The data for compounds **3**–**6** and **11** were corrected for absorption using the program DIFABS[26] with maximum and minimum correction factors listed in Table 8. An absorption correction could not be successfully applied to **1** due to the weakness of the data set. The non-hydrogen atoms were refined with anisotropic thermal parameters. All of the hydrogen atoms in compounds **1**, **4**–**6** and **11** were included in idealised positions. The phenyl hydrogens of **3** were experimentally located, whilst the methyl hydrogens of the *tert*-butyl groups were placed in calculated positions. Fractional atomic coordinates are given in Tables 9–14.

Complete atomic coordinates, thermal parameters and bond lengths and angles have been deposited at the Cambridge Crystallographic Data Centre. See Instructions for Authors, *J. Chem. Soc., Dalton Trans.*, 1996, Issue 1.

Acknowledgements

We thank the EPSRC for support (to A. A. D.) and provision of X-ray facilities.

References

1 T. Zincke and J. Baeumer, *Liebigs Ann. Chem.*, 1918, **416**, 86.
2 *The Chemistry of Sulphenic Acids and Their Derivatives*, ed. S. Patai, Wiley, Chichester, 1990.
3 *Chem. Eng. News*, 1994, 29 Aug., p. 11.
4 E. K. Haub, J. Richardson and M. E. Noble, *Inorg. Chem.*, 1992, **31**, 4926.
5 A. A. Danopoulos, G. Wilkinson, B. Hussain and M. B. Hursthouse, *J. Chem. Soc., Dalton Trans.*, 1990, 2753; A. A. Danopoulos, G. Wilkinson, T. K. N. Sweet and M. B. Hursthouse, *Polyhedron*, 1994, **13**, 2899.
6 D. M. Hankin, A. A. Danopoulos, G. Wilkinson, T. K. N. Sweet and M. B. Hursthouse, *J. Chem. Soc., Dalton Trans.*, 1995, 1059.
7 See, for example, B. F. G. Johnson, B. L. Haymore and J. R. Dilworth, in *Comprehensive Coordination Chemistry*, eds. G. Wilkinson, R. D. Gillard and J. A. McCleverty, Pergamon, Oxford, 1987, vol. 2.
8 D. A. Armitage, M. J. Clark and A. C. Kinsey, *J. Chem. Soc. C*, 1971, 3867.
9 G. Capozzi, G. Modena and L. Pasquato, in *The Chemistry of Sulfenic Acids and Their Derivatives*, ed. S. Patai, Wiley, Chichester, 1990, p. 414.
10 Y. Miura and M. Kinoshite, *Bull. Chem. Soc. Jpn.*, 1977, **50**, 1743.
11 C. Paulmier, P. Lerouge, F. Outurquin, S. Chapelle and P. Granger, *Magn. Reson. Chem.*, 1987, **25**, 955.
12 E. W. Abel, S. K. Bharogava and K. G. Orrell, *Prog. Inorg. Chem.*, 1984, **32**, 1 and refs. therein.
13 A. S. Ward, E. A. Mintz and M. R. Ayers, *Organometallics*, 1986, **5**, 1585.
14 A. A. Danopoulos, A. C. C. Wong, G. Wilkinson, B. Hussain-Bates and M. B. Hursthouse, *J. Chem. Soc., Dalton Trans.*, 1990, 315.
15 A. A. Danopoulos, G. Wilkinson, B. Hussain-Bates and M. B. Hursthouse, *J. Chem. Soc., Dalton Trans.*, 1990, 2753.
16 F. M. Chung and A. D. Westland, *Can. J. Chem.*, 1969, **47**, 195.
17 B. Kamenar, M. Penavic, B. Korpar-Colig and B. Markovic, *Inorg. Chim. Acta*, 1982, **65**, L245.
18 K. Dreisch, C. Andersson and C. Stalhandske, *Polyhedron*, 1991, **10**, 2417.
19 G. Schoettel, J. Kress and J. A. Osborn, *J. Chem. Soc., Chem. Commun.*, 1989, 1062.
20 J. Sundermeyer, *Chem. Ber.*, 1991, **124**, 1977.
21 (*a*) A. G. M. Barrett, D. Dhanak, G. G. Graboski and S. J. Taylor, *Org. Synth.*, 1990, **68**, 8; (*b*) R. Pitteloud and M. Petrilka, *Helv. Chim. Acta*, 1979, **62**, 1319.
22 F. Bottino, R. Fradullo and S. Pappalardo, *J. Org. Chem.*, 1981, **46**, 2793.
23 A. A. Danopoulos, G. Wilkinson, B. Hussain-Bates and M. B. Hursthouse, *J. Chem. Soc., Dalton Trans.*, 1991, 1855.
24 G. M. Sheldrick, SHELXS 86, *Acta Crystallogr., Sect. A*, 1990, **46**, 467.
25 G. M. Sheldrick, SHELXL 93, Program for Crystal Structure Refinement, University of Göttingen, 1993.
26 N. P. C. Walker and D. Stuart, *Acta Crystallogr., Sect. A*, 1983, **39**, 158 (adapted for FAST geometry by A. Karaulov, University of Wales, Cardiff, 1991).

Received 18*th October* 1995; *Paper* 5/06901G